International Journal of Theoretical and Applied Physics (IJTAP),
ISSN: 2250-0634, Vol. 7, No. I (December 2017), pp. 1-11

CHAOS, HYSTERESIS AND VIBRATIONAL RESONANCE IN A SINGLE SCROLL CHUA'S CIRCUIT DRIVEN BY FREQUENCY MODULATED FORCE

V. BALA SHUNMUGA JOTHI [1], S. SELVARAJ [1], V. CHINNATHAMBI [2*] AND S. RAJASEKAR [3]

[1]Department of Physics, The M.D.T.Hindu College, Tirunelveli 627 012, Tamilnadu, India.
[2]Department of Physics, Sadakathullah Appa College, Tirunelveli 627 011, Tamilnadu, India.
[3] School of Physics, Bharathidasan University, Thiruchirapalli 620 024, Tamilnadu, India.

Abstract

We numerically examine the effect of frequency modulated force (FMF) on a single scroll Chua's piecewise - linear circuit. Under the action of such a force, this circuit exhibits a large variety of bifurcation sequence including period-doubling, windows in chaotic regime, routes to chaos, crises, hysteresis and vibrational resonance phenomena for a specific set of values of the parameters of the system. In addition, control of chaos can be effected in this circuit. We characterize periodic, quasiperiodic and chaotic events using bifurcation diagram, phase portrait, trajectory plot and Poincare surface of section plot.

Keywords: Chua's circuit, Hysteresis, Chaos, Vibrational resonance, Frequency modulated force

1. INTRODUCTION:

Chua's circuit is the simplest autonomous generator of chaotic signals and is surely one of the most extensively studied chaotic circuits because of its simple circuit topology. Chua's circuit is of unique significance and for several reasons represents a milestone in the research on chaos theory and application [1-5]. Since its discovery in 1984, Chua's circuit has been studied extensively. A number of experimental, numerical and theoretical investigations have been carried out on this circuit to study the various nonlinear phenomena for various parametric choices [6-14].

In many nonlinear circuits and systems, rich dynamics has been found due to the coexistence of several attractors. The coexistence of several attractors gives rise to the possibility of

hysteresis and is encountered in many scientific fields, including magnetism, superconductor, granular media and population dynamics. Some characteristic examples exhibit hysteresis such as one-dimensional map model [15], Ueda oscillator [16], two coupled over damped anharmonic oscillator [17], Colpitt's oscillator [18] and modified Chua's circuit model [19].

The phenomenon of vibrational resonance (VR) in which the response of the system to a weak periodic signal can be enhanced by the application of a high frequency periodic perturbation of appropriate amplitude. The analysis of VR has received a considerable interest in recent years because of its importance in a wide variety of contents in physics, engineering and biology. The occurrence of this resonance has been analyzed theoretically [20-22], numerically [23-25] and experimentally [26-28]. It has also been thoroughly studied in a large class of dynamical systems such as a monostable system [29], a multistable system [30], time-delayed system [31,32], spatially periodic potential system [33], small world networks [24,25] and nonlinear maps [34,35].

In the present work, we wish to numerically analyze chaos, hysteresis and vibrational resonance phenomena in a single-scroll Chua's circuit driven by FMF . The single-scroll Chua's circuit driven by FMF is given by the following closed form dimensionless equations:

$$\begin{aligned} \dot{x} &= a\,(y - f(x)) + f\sin(\omega t + g\cos\Omega t) \\ \dot{y} &= x - y + z \\ \dot{z} &= -by \end{aligned} \tag{1}$$

where f is the unmodulated carrier amplitude, g is the modulation index, ω and Ω are the two frequencies of the external force with $\Omega >> \omega$ and a and b are constant parameters. Here $f(x)$ represents the piece-wise linear function,

$$f(x) = cx + \frac{1}{2}(d-c)(|x+1| - |x-1|) \tag{2}$$

where c and d are constant parameters. Recently, Lai et al. [36] investigated the possibility of suppression of jamming and stochastic resonance by both narrow band and wide band frequency modulated signals in FitzHuge-Nagumo oscillator and Lorenz equations. Also,

Ravisankar et al. [37] investigated both analytically and numerically the effect of narrow - band frequency modulated force on horseshoe chaos in Duffing-vander Pol oscillator. This paper is organized as follows. In the next section, the dynamics of this system is analyzed by numerical simulations including bifurcations of chaos, routes to chaos, vibrational resonance and transient chaos. Finally we summarize the results and indicate future directions.

2. **DYNAMICAL BEHAVIOURS OF THE SYSTEM (1):**

In this section we numerically investigate certain dynamical behaviours of the system (1) such as bifurcations of periodic orbits, routes to chaos, hysteresis and vibrational resonance. Throughout our numerical study, we fix parameter values as $a = 7.0$, $b = 14.286$, $c = 2/7$, $d = -1/7$, $\omega = 3.5$ and $\Omega = 10.5$ and choose the period of the force as $2\pi/\omega$. Equation (1) is solved by the fourth order Runge-Kutta method with time step size $(2\pi/\omega)/200$, with the initial conditions $x = 1.54$, $y = -0.3138$ and $z = -2.73$. Numerical solution corresponding to first 500 drive cycles is left as transient. We analyzed the behaviours of the system (1) by varying the amplitudes f and g and the frequency ω of the FMF.

2.1 HYSTERESIS:

Before studying the system (1) in the presence of both low - and high - frequency forces, we consider the system with the low - frequency force alone ($g = 0$) respectively the high - frequency force alone ($f = 0$). When $g = 0$, the system (1) is driven by the sinusoidal force f sinωt. Hysteresis is realized when f is varied in the forward and reverse directions in the interval $f \in [0, 2]$. Bifurcation diagrams plotted by varying f in the forward direction as well as reverse direction with the above initial conditions are shown in Fig. 1.

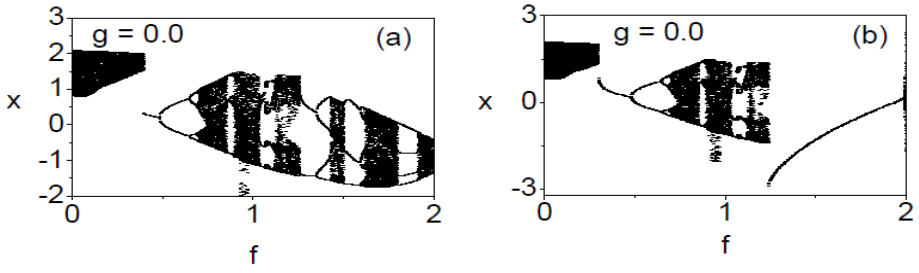

Fig.1: Bifurcation diagrams. (a) Varying the amplitude f from 0 in the forward direction (b) Varying f in the reverse direction from the value 2.

Figure 1(a) is obtained by varying the amplitude f from a small value in the forward direction. Fig.1(b) is obtained by varying f in the reverse direction from the value 2. Different paths are followed in the Figs. 1(a) and (b). That is, the system exhibits hysteresis when the control parameter f is varied smoothly from a small value to a larger one and then back to a small value.

When we consider the system in the presence of the high-frequency force alone, that is $f = 0$ no hysteresis is found. At $f = 0$, the system becomes an unperturbed system. Next we consider the effect of high-frequency force on the response of the system (1) in the presence of the low- frequency force ($f \neq 0$ and $g \neq 0$) . We fix $f = 0.5$, $\omega = 3.5$ and $\Omega = 10.5$. For these values of the parameters in the absence of high - frequency force ($g = 0$), we get period-2T orbit. We now study the response of the system (1) by varying the amplitude g of the high-frequency force. Figures 2(a) and (b) show the bifurcation diagrams obtained by varying g in the forward and reverse directions respectively. Different paths are followed when g is varied along forward and reverse directions. We can clearly notice a hysteresis in Fig. 2. The system (1) is also found to show reverse period-doubling, quasiperiodic orbit and reverse periodic windows in addition to hysteresis.

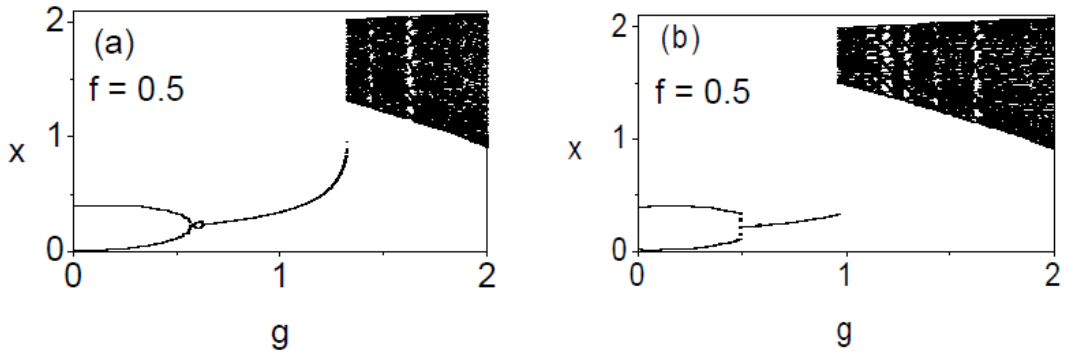

Fig. 2: Bifurcation diagrams showing hysteresis phenomenon. (a) Bifurcation sequence when g is varied from 0 to 2. (b) Bifurcation sequence when g is decreased from 2 to 0.

2.2 VIBRATIONAL RESONANCE:

From the numerical solution of $x(t)$, the response amplitude Q is computed through

$Q=\sqrt{Q_S^2+Q_C^2}\,/\,f$ and the phase shift Ψ = -arctan (Q_S/Q_C) of the response relative to the input signal, where

$$Q_S=\frac{2}{MT}\int_0^{MT}x(t)\sin\omega t\,dt, \qquad 3(a)$$

$$Q_C=\frac{2}{MT}\int_0^{MT}x(t)\cos\omega t\,dt, \qquad 3(b)$$

where T = 2π/ω and M is taken as 500. Q_S and Q_C measure the coefficients of the Fourier sine and cosine components respectively of the output signal at the frequency 2π/*T*. Q measures the amplitude of the response at the frequency 2π/*T*. Figure 3(a) presents the numerically computed response amplitude Q versus *g* for *f* = 0.5, ω = 3.5 and Ω = 10.5. As *g* increases the resultant amplitude Q increases and reaches a maximum value at g = g_{max} = 1.25 but then decreases with further increase in *g*. This phenomenon is the VR, since the occurrence is due to high - frequency force. The variation of the phase shift ψ with the amplitude *g* of the high - frequency vibrational force is shown in Fig. 3(b). Though the period of the orbit in the entire range of *g* is T (= 2π/ω) the response has distinct qualitative and quantitative characteristics in the regions-I, II and III. We use the tools such as phase portrait and trajectory plot to describe the dynamics in these regions. The phase portraits of the regions-I, II and III at *g* = 0.5, 1.12 and 1.75 are shown in Fig. 4. The corresponding trajectory plot of orbits in the regions I, II and III at *g* = 0.5, 1.12 and 1.75 are shown in Fig.5

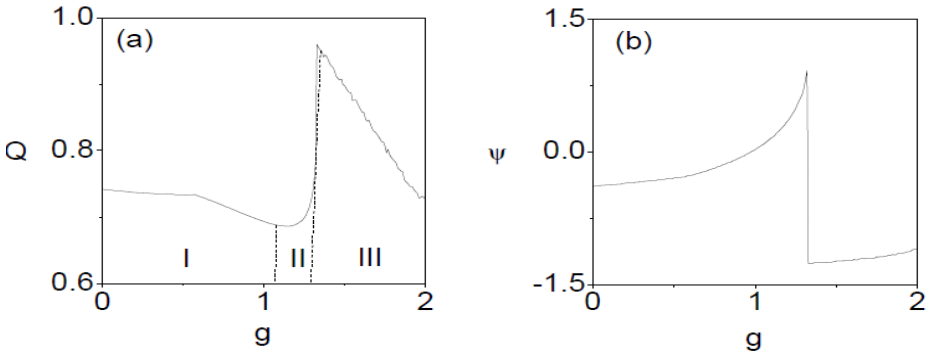

Fig.3 (a) Variation of numerically computed Q against the control parameter *g*.

(b) The variation of phase shift ψ with the amplitude of high frequency force *g*.

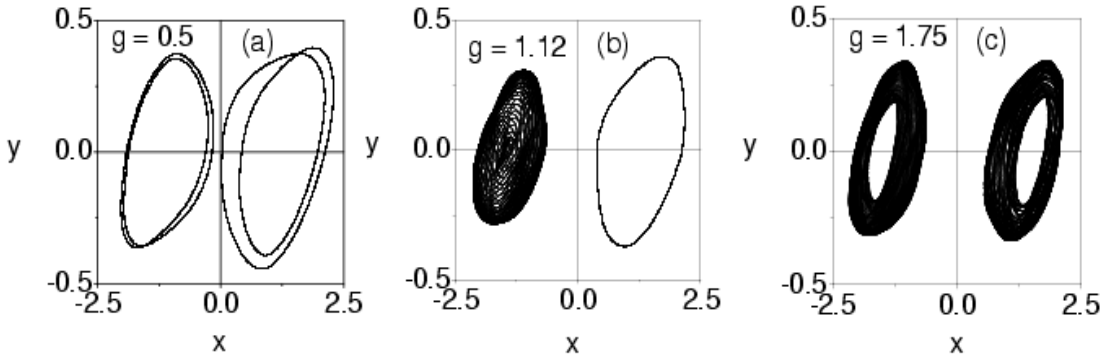

Fig.4 Phase portraits of the system (1) driven by FMF for choosing the values from region-I, II, III in Fig.3.

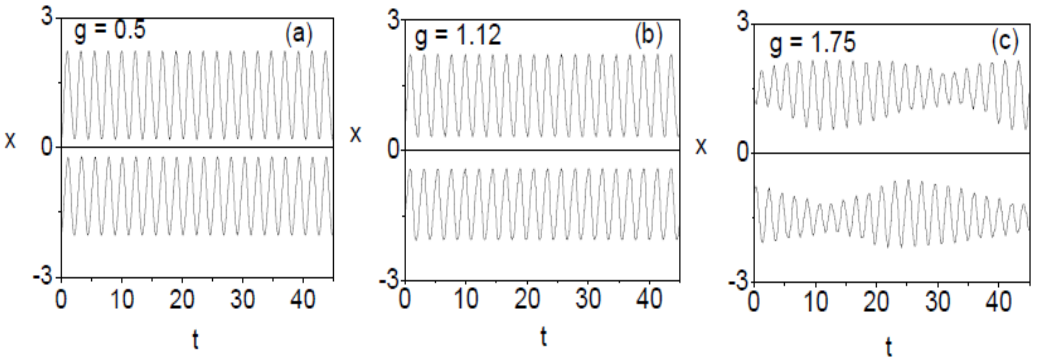

Fig.5 The trajectory plots for the three regions in Fig.3

Next, we analyze the influence of the parameters f and ω on resonance. Figure 6 presents the results. In Fig. 6(a), we observed the effect of increasing the values of f such as f = 0.2, 0.3, 0.4. 0.5, 0.6 with ω = 3.5 and Ω = 10.5. Single resonance occurs for f = 0.6 and no resonance occurs for f = 0.2, 0.3, 0.4 and 0.5. In Fig.6(b), $Q(g)$ is plotted for different values of ω, such as ω = 0.1, 0.3, 0.5, 1.5, 3.5 and keeping the value of Ω as 10.5, that is decreasing the ratio of Ω/ω. For ω = 3.5, single resonance occurs and no resonance occurs for ω = 0.1, 0.3, 0.5 and 1.5.

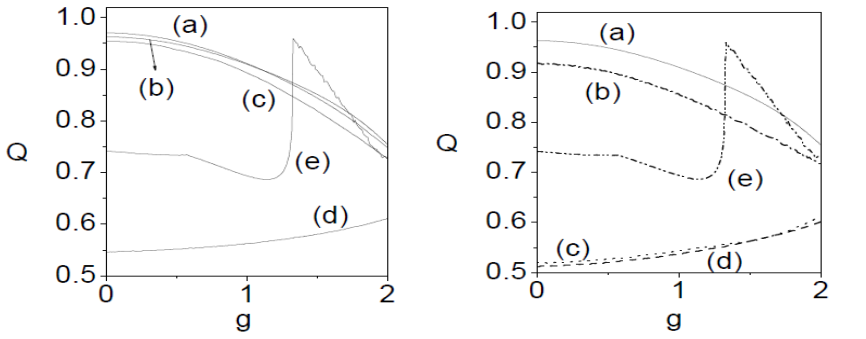

Fig.6 (i) Response amplitude Q versus g for five values of f. The values of f for (a), (b), (c), (d) and (e) lines are 0.2, 0.3, 0.4, 0.5 and 0.6 respectively. (ii) Response amplitude Q versus g for five values of ω. The values of ω for (a), (b), (c), (d) and (e) lines are 0.1, 0.3, 0.5, 1.5 and 3.5 respectively.

2.3 REGULAR AND CHAOTIC MOTIONS OF SYSTEM (1)

Since the system (1) can exhibit variety of bifurcations of periodic orbits leading to chaotic motion and bifurcation of chaotic attractor, we examined the occurrence of them using bifurcation diagram, phase portrait and Poincare map. For certain cases of parametric choices considered in our study, routes to chaos, crises and chaotic motion are found for sufficiently large values of the control parameter g. An example is presented in Fig. 7. We fix the values of the parameter as a = 7.0, b = 14.286, c = 2/7, d = -1/7, ω = 3.5 and Ω = 10.5. Figure 7(a) shows the bifurcation diagram where g is set to zero while f is varied. As f is increased from zero, a quasiperiodic orbit occurs which persists up to f = 0.4 and then it loses its stability giving birth to a period-T orbit. System (1) then undergoes further period doubling bifurcations as the control parameter f is smoothly varied. For example at f = 0.64830, the period-2T orbit becomes unstable and gives birth to period-4T orbit. This cascade of bifurcation continues further as 8T, 16T…, orbits and accumulates at $f = f_c$ = 0.70723. At this critical value of f onset of chaotic motion occurs. When the parameter f is further increased from f_c one finds that chaotic orbits persist for a range of f values interspersed by periodic windows, period - doubling windows, crises and intermittency routes to chaos.

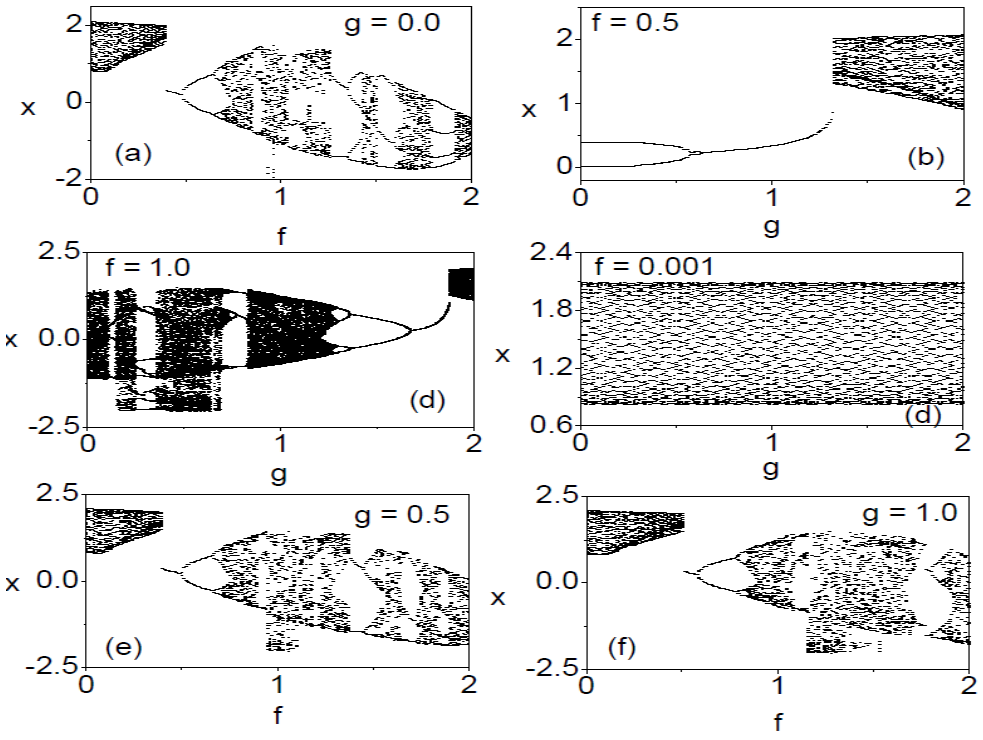

Fig.7 Bifurcation structures of the system (1) for various values of f and g values.

We show the effect of the control parameter g by fixing the values of f in a regular region and then in a chaotic region. For $f = 0.5$ and $g = 0$ the motion of the system is periodic with period - $2T$. Figure 7(b) is the bifurcation diagram obtained by varying g from 0 to 2. As g is increased from zero the reverse period-$2T$ orbit persists upto $g = 0.5$ and then period-T solution is developed. This is followed by quasiperiodic orbit. Figure 7(c) corresponds to $f = 0.8$ (Chaotic motion when $g = 0$). When the control parameter g is smoothly varied, system (1) starts with chaotic motion followed by reverse period doubling bifurcation and quasiperiodic orbit. Periodic behaviour is observed in the interval $1.25 < g < 1.75$. That is the parameter g can be used to suppress chaotic motion by choosing its value in this interval.

The bifurcation diagram corresponding to $f = 0.001$ and $g \in [0, 2]$ is shown in Fig. 7(d). The influence of the control parameter f on the dynamics of the two fixed values of g, namely $g = 0.5$ and 1.0 is also studied. The effect of f can be clearly seen in Figs. 7(e) and (f). Bifurcation patterns in Figs.7(e) and (f) are almost identical. Here again suppression and enhancement of chaos is found for certain range values of the control parameter f. For

clarity an example of quasiperiodic orbit, limit cycle and chaotic attractor from Fig.7 is shown in Fig. 8

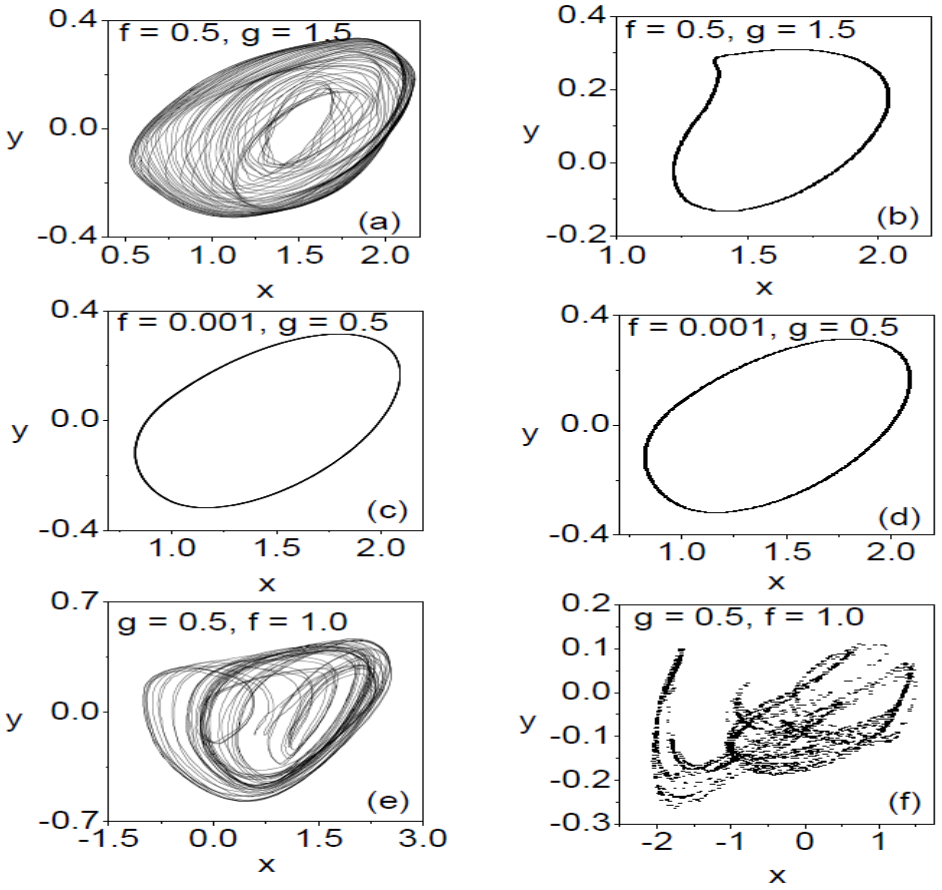

Fig.8: Phase portraits and the corresponding Poincare maps of the system (1). (a-b) Quasiperiodic orbit (c-d) Limit cycle and (e-f) Chaotic attractor.

3. CONCLUSION:

In the present paper, we numerically studied the dynamics of a single-scroll Chua's circuit driven by frequency modulated force (FMF) for specific set of values of the parameters. Hysteresis and vibrational resonance phenomena are found. Various types of bifurcations and routes to chaos are encountered in the system (1). The frequency modulated force which we encountered in the present work has four parameters such as *f*, *g*, ω and Ω. As shown in Fig. 7 the presence of additional parameters can be used to control and anti - control of chaos. It is important to study the various nonlinear phenomena including ghost - vibrational

resonance, coherence resonance and stochastic resonance in the presence of FMF. These will be investigated in future.

REFERENCES.

[1] Chua L.O., The genesis of Chua's circuit, Archiv f$\ddot{U}$rElectronik and $\ddot{U}$bertragungstechnik 46, 250 (1992).

[2] Madan R.N., Chua's circuit : A paradigm for chaos (World Scientific, Singapore, 1993).

[3] Pospisil J., Kolka Z. and Brzobohaty J., Int. J. Bifur. and Chaos 10(1), 1 (2000).

[4] Lakshmanan, M. and Murali K., Chaos in nonlinear oscillators, controlling and Synchronization (World Scientific, Singapore, 1996).

[5] Chen G. and Ueda T., Chaos in circuits and systems (World Scientific, Singapore, 2002).

[6] Fortuna L., Frasca M. and Xibilia M.G., Chua's circuit implementations : Yesterday, Today and Tomorrow (World Scientific, Singapore, 2009).

[7] Kilic R., A Practical Guide for studying Chua's circuits (World Scientific, Singapore, 2010).

[8] Sakthivel G., Rajasekar S., Thamilmaran K. and Dana S.K., Int. J. Bifur. and Chaos 22, 1250004 (2012).

[9] Arathi S., Rajasekar S. and Kurths J., Int. J. Bifur. and Chaos 23, 1350132 (2013).

[10] Buscarino A., Fortuna L. and Frasca M., Int. J. Bifur. and Chaos 19, 2557 (2009).

[11] Chakraborty S. and Dana S.K., Chaos 20, 023107 (2010).

[12] Gomes I., Vermelto M.V.D., Lyra M.C., Phys. Rev. E 85, 056201 (2012).

[13] Heo Y.S., Jung J.W., Kim J.M., Jo M.K. and Song H.J., Journal of Korean Phys. Soc. 60,1140 (2012).

[14] Borreson J. and Lynch S., Int. J. of Bifur. and Chaos 12(1), 129 (2002).

[15] Back S.K. and Moon H.T., Phys. Lett. A 352(1), 89 (2006).

[16] Sun K., Di-li Duo Li-Kum A., Dong Y., Wang H. and Jhong Ki., Hindawi Publishing corporation, Mathematical problems in Engineering, Vol.2013, Article ID: 256092 (7 pages).

[17] Gandhimathi V.M., Rajasekar S. and Kurths J., Phys. Lett. A 360, 279 (2006).

[18] deFeo O. and Mario Maggio G., Int. J. Bifur. and Chaos 13, 2917 (2003).

[19] Abirami K., Rajasekar S. and Sanjuan M.A.F., arXiv: 1406. 68336 v1 [nlin.CD] 26 June 2014.

[20] Landa P.S. and McClintock P.V.E., J. Phys. A: Math. Gen. 33, L433 (2000).

[21] Gitterman M., J. Phys. A: Math. Gen. 34, L355 (2001).

[22] Chizhevsky V.N., Int. J. Bifur. and Chaos 18, 1767 (2008).

[23] Ullner E., Zaikin A, Garcia – Ojalvo J., Bascones R. and Kurths J, Phys. Lett. A 312, 348 (2003).

[24] Dang B., Wang J and Wei X, Chaos 19, 013117 (2009).

[25] Dang B., Wang J., X.Wei X., Jsang K.M. and Chan W.L., Chaos 20, 013113 (2010).

[26] Baltanas J.P., Lopez L., Blekhman I.I., Landa P.S., Zaikin A., Kurths J. and SanjuanM.A.F.,Phy. Rev. E 67, 066119 (2003).

[27] Chizhevsky V.N. and Giacomelli G., Phys. Rev. E 73, 022103 (2006).

[28] Chizhevsky V.N. and Giacomelli G., Phys. Rev. E 77, 051126 (2008) .

[29] Jeyakumari S., Chinnathambi V., Rajasekar S. and Sanjuan M.A.F., Phy. Rev. E 80, 046608, (2009).

[30] Jeyakumari S., Chinnathambi V., Rajasekar S. and Sanjuan M.A.F., Chaos 19, 043128 (2009).

[31] Jeevarathinam C., Rajasekar S. and Sanjuan M.A.F., Phys. Rev. E 83, 066205 (2011).

[32] Daza A., Wagemakers A., Rajasekar S. and Sanjuan M.A.F., Commun.Nonlinear Sci.Numer.Simulat. 18, 411 (2013).

[33] Rajasekar S., Abirami K. and Sanjuan M.A.F., Chaos 21, 033106 (2011).

[34] Rajasekar S., Used J., Wagemakers A.and Sanjuan M.A.F., Commun.Nonlinear Sci.Numer.Simulat. 17, 3435 (2012).

[35] Jeevarekha A., Santhiah M. and Philominathan P., Pramana J.of Physics 83(4), 493 (2014).

[36] Lai Y.C., Liu Z., Nachman A. and Zhu L., Int. J. Bifur. and Chaos 14, 3519 (2004).

[37] Ravisankar L., Ravichandran V., Chinnathambi V. and Rajasekar S., IJSER 4 (8), 1 (2013).